Journal of Pharmaceutical Sciences 105 (2016) 1258–1268

Contents lists available at ScienceDirect

Journal of Pharmaceutical Sciences

journal homepage: www.jpharmsci.org

Pharmaceutics, Drug Delivery and Pharmaceutical Technology

Preparation and Physical Characterization of a Diclofenac-Ranitidine Co-precipitate for Improving the Dissolution of Diclofenac

Robertino O. Gaitano [1], Natalia L. Calvo [2], Griselda E. Narda [1], Teodoro S. Kaufman [2], Rubén M. Maggio [2,*], Elena V. Brusau [1,*]

[1] *Química Inorgánica, Departamento de Química, Facultad de Química, Bioquímica y Farmacia, Universidad Nacional de San Luis and Instituto de Investigaciones en Tecnología Química (INTEQUI, CONICET-UNSL), San Luis D5700BWQ, Argentina*
[2] *Análisis Farmacéutico, Departamento de Química Orgánica, Facultad de Ciencias Bioquímicas y Farmacéuticas, Universidad Nacional de Rosario and Instituto de Química Rosario (IQUIR, CONICET-UNR), Rosario S2002LRK, Argentina*

ARTICLE INFO

Article history:
Received 9 October 2015
Revised 4 December 2015
Accepted 5 January 2016
Available online 9 February 2016

Keywords:
ranitidine
diclofenac
co-crystal
FTIR
NMR spectroscopy
physical characterization
solid-state
dissolution
chemometrics

ABSTRACT

Mixing aqueous solutions of sodium diclofenac (DIC-Na) and ranitidine hydrochloride (RAN·HCl) afforded an off-white solid (DIC-RAN) that was investigated from the microscopic, thermal, diffractometric, spectroscopic, and functional (chemometrics-assisted dissolution) points of view. The solid has a 2:1 (DIC:RAN) molar ratio according to ^{1}H nuclear magnetic resonance spectroscopy. It is thermally stable, displaying a broad endothermic signal centered at 105°C in the thermogram, and its characteristic reflections in the powder X-ray diffractogram remained unchanged after a 3-month aging period. Scanning electron microscopy micrographs uncovered its morphology, whereas the spectral data suggested an interaction between the carboxylic acid of DIC and the alkyldimethylamino moiety of RAN. The dissolution of DIC-RAN was monitored at different pH values by an ultraviolet/chemometrics procedure, being complete within 5 min at pH 6.8. This compares favorably with the dissolution of a DIC-Na sample of the same particle size.

Introduction

The delivery of active pharmaceutical ingredients (APIs) with poor aqueous solubility is a current challenge because the oral bioavailability depends on their dissolution rate in the absorption site. Various formulation or processing-based approaches have been devised to increase the solubility of poor water-soluble drugs; however, one of the most convenient strategies toward this purpose is the improvement of their physicochemical properties.

Diclofenac (DIC, Fig. 1) is 2-[(2′,6′-dichlorophenyl)amino] benzeneacetic acid, a potent nonsteroidal anti-inflammatory agent, with pronounced antipyretic and analgesic properties, which is widely used in the long-term treatment of degenerative joint diseases. DIC is an acidic drug, which has very low aqueous solubility in its unionized form (6×10^{-5} M at 25°C),[1] being practically insoluble in HCl solutions at pH 1.1, very slightly soluble in phosphate buffer at pH 6.8, and slightly soluble in pure H_2O.[2]

DIC has 3 hydrogen bond acceptors, 2 hydrogen bond donors, and significant conformational flexibility; however, the carboxylic acid moiety and the secondary amino group of DIC are the sources of tight intra- and intermolecular H-bonds, which generate a dimeric centrosymmetric structure, and cause the high melting point of the drug. This dimeric form, where all the H-bonds involve inter- and intramolecular hydrophilic groups, represents the structural unit of the solid state of DIC, which turns the drug less available to intermolecular interactions with water, the result being its poor aqueous solubility.

On the other side, ranitidine (RAN, Fig. 1) is *N*-{2-[[[5-[(dimethylamino)methyl]-2-furanyl] methyl]thio]ethyl}-*N*′-methyl-2-nitro-1,1-ethenediamine. The drug is a histamine H2-receptor antagonist that inhibits the secretion of gastric acid induced by various stimuli, while lacking unwanted antiandrogenic and hepatic microsomal enzyme-inhibiting effects.

This article contains the supplementary materials FTIR spectral comparisons (KBr vs. DRIFTS and physical mixture vs. DIC-RAN), chemical structures of DIC and RAN, and ^{13}C NMR spectra of RAN·HCl, RAN, DIC-Na, and DIC-RAN available from the authors by request or via the Internet at http://dx.doi.org/10.1016/j.xphs.2016.01.001.

* *Correspondences to:* Rubén M. Maggio (Telephone/Fax: +54-341-4370477) and Elena V. Brusau (Telephone/Fax: +54-266-4520300).
E-mail addresses: maggio@iquir-conicet.gov.ar (R.M. Maggio), ebrusau@unsl.edu.ar (E.V. Brusau).

http://dx.doi.org/10.1016/j.xphs.2016.01.001
0022-3549/

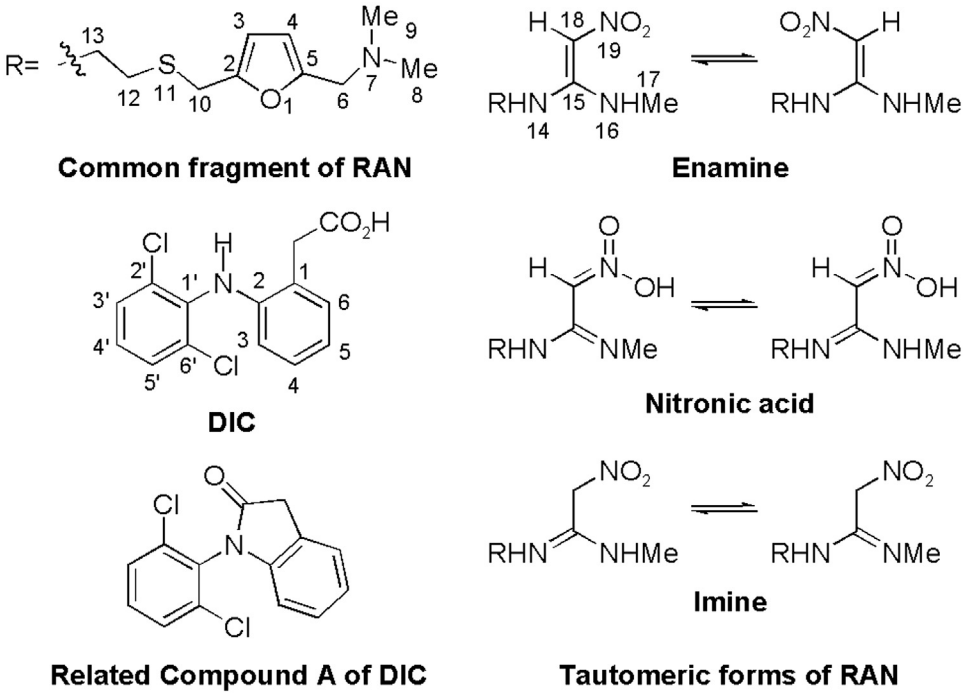

Figure 1. Chemical structures of DIC, the related compound A of DIC, and the tautomeric forms of RAN.

RAN is a dibasic drug, commercially available as the monohydrochloride salt (ranitidine hydrochloride [RAN·HCl]), which is highly soluble in water. Theoretically, it can exist in 3 main tautomeric forms (imine, enamine, and nitronic acid; see Fig. 1). In addition, the enamine could exist as 2 geometrical (*E*/*Z*) isomers, and the nitronic acid and imine forms could both exhibit further prototropic tautomerism within the amidine group and *syn-anti*-isomerism about the C-N bonds. This tautomer interconversion requires 1,5- or 1,3-proton shifts,[3] analogous to those proposed for cimetidine.[4]

RAN·HCl has 2 known polymorphs (forms 1 and 2). The structure of form 2, solved by single crystal X-ray diffraction (XRD), exhibits molecular disorder in the nitroethenediamine moiety. The structural data suggest contributions, 50% each, from the nitronic acid and the enamine tautomers. On the other hand, nuclear magnetic resonance (NMR) studies revealed that form 1 does not show molecular disorder, hinting that a single tautomer is present in the solid.[5]

It has been suggested that in aqueous solutions, the geometrical isomers are in rapid equilibrium, in the NMR time scale, affecting the resonances of H-17 and H-18, which result in broad signals.[6] However, on protonation of the diaminovinyl group, the interconversion of the *E* and *Z* species is slowed down on account of the formation of intramolecularly H-bonded species.

It is well established that the solubility and the bioavailability of poorly water-soluble drugs can be improved by converting them into the amorphous state.[7] On the other hand, co-precipitate systems resulting from the interaction of 2 chemical entities to form a single-phase system usually exhibit improved physical stability and aqueous dissolution profile, compared with the individual drugs.[8]

It is also known that salt formation is a very simple and straightforward chemical tool, commonly used for enhancing the solubility and dissolution rate of poorly soluble drugs containing ionizable functional groups.[9] In this case, the nature of the counterion is relevant to both the processability of the product and its physicochemical characteristics, including solubility, dissolution rate, and stability. In all cases, the intermolecular interactions between the components of the system have been pointed out as responsible for the observed improvements.

Because of its wide use, various strategies have been used to enhance the solubility and dissolution rate of DIC. One of them consists in the elaboration of derivatives of the APIs, such as salts,[10,11] co-crystals,[12] ionic pairs,[13] and complexes with cyclodextrins.[14] Another alternative entails modifying the vehicle, in this approach, including the use of mixed solvency,[15,16] formation of liquisolids,[17] solid dispersions,[18] nanosuspensions,[19] micellar dispersions and microemulsions,[20] and inclusion in supramolecular matrices,[21] among others.

Various salts of DIC are currently part of pharmaceutical products, including sodium, potassium, and ammonium derivatives, and diclofenac *N*-(2-hydroxyethyl)pyrrolidine and diclofenac diethylamine.[22] In addition, a screening toward co-crystals of DIC has been recently reported.[23]

It has been shown that RAN is able to protect against the ulcerogenic effect of nonsteroidal anti-inflammatory agents, such as DIC. Therefore, these active principles are frequently administered. Furthermore, the pharmacologic interaction between DIC and RAN has been studied *in vivo*, concluding that it is minimal and that the attained gastric pH range did not influence the oral absorption of enteric-coated diclofenac.[24]

In addition, it has been observed that the concomitant intake of RAN has no effect on the pharmacokinetics of DIC.[25] Bilayer tablets containing a fixed-dose combination of DIC and RAN have recently been evaluated,[26] and the bioavailability of a formulation containing DIC and RAN has also been studied.[27]

Previous studies on the chemical interaction between DIC and RAN were also unable to detect any effect.[28] As DIC is an acidic drug and RAN is a basic pharmaceutical ingredient, we were puzzled about this intriguing observation; therefore, we decided to assess if this finding was correct. As a result, here we report the preparation and characterization (spectroscopic, thermal, structural, and morphologic) of an off-white microcrystalline solid (DIC-RAN).

Finally, a complete functional evaluation in the dissolution test of the co-crystal was performed.

Experimental Section

Materials

All the experiments were performed with pharmaceutical-grade sodium diclofenac (DIC-Na; Prozome Laboratories) and RAN·HCl (Inmobal Nutrer Laboratories), both kindly provided by the "Laboratorio de Control de Calidad de Medicamentos," Universidad Nacional de San Luis, Argentina. Water was obtained from a Milli-Q System (Millipore, Bedford, MA) and used for preparing the samples and dissolution media. All other chemicals were of analytical grade and were used as received.

Preparation of DIC-RAN

Aqueous solutions of DIC-Na (15 mL, 0.07 M) and RAN·HCl (5 mL, 0.2 M) were mixed under stirring at 50°C. This immediately resulted in the appearance of an off-white solid (DIC-RAN), which was filtered, washed with distilled water, and dried at ambient conditions for further characterization and use. The yield of the solid product was 20%.

In addition, a physical mixture of RAN·HCl and DIC-Na was prepared by mixing to homogeneity accurately weighed amounts of both APIs to keep the same molar relationship used in the preparation of DIC-RAN.

Melting Point Determination

The melting behavior of DIC-RAN was examined at a hot stage (hot-stage microscopy [HSM]) using a Leitz-Wetzlar microscope.

Thermogravimetric Analysis

The thermal degradation of DIC, DIC-Na, RAN·HCl, and DIC-RAN was measured with a Shimadzu TGA-51 thermal analyzer (Shimadzu Corp., Kyoto, Japan). The samples were heated at a rate of 10°C per minute under air at a flow rate of 50 mL min^{-1}.

Differential Scanning Calorimetry

The investigation of the thermal properties of DIC-RAN and its precursors was carried out on a Shimadzu DSC-60 thermal analyzer (Shimadzu Corp.). Each sample was placed in a 40-μL aluminum pan and covered with a perforated aluminum lid. An empty pan was used as reference. The instrument was calibrated for temperature using indium as a standard. For better comparisons, the differential scanning calorimetry (DSC) and thermogravimetric analysis (TGA) experiments were conducted with almost identical amounts of DIC, DIC-Na, RAN·HCl, and DIC-RAN.

Fourier Transformed Infrared

The Fourier transformed infrared (FTIR) spectra were recorded on a Nicolet 460 Protégé spectrometer (Nicolet Instrument Corp., Madison, WI) in the transmittance mode, using the KBr pellet technique. The diffuse reflectance infrared Fourier transform spectroscopy (DRIFTS) spectrum of DIC-RAN was obtained with the same IR spectrometer, equipped with a Spectra-Tech 60 series Magna accessory (Spectra-Tech Inc., Shelton, CT). The sample was dispersed by geometric mixing with KBr to yield a 5% wt/wt mixture. An average of 64 scans was used at a 4 cm^{-1} resolution in all cases, between 4000 and 600 cm^{-1}.

Powder X-Ray Diffraction

The crystallinity of DIC-RAN was evaluated with a Rigaku D-Max-IIIC (Rigaku Corp., Tokyo, Japan) X-ray diffractometer, using Cu K_α radiation ($\lambda = 1.5418$ Å, Ni filter). NaCl and quartz were used as external calibration standards. Diffraction intensities were measured in the range of 5-50° (2θ degrees).

Scanning Electron Microscopy

Scanning electron microscopy (SEM) was used to observe and analyze the morphology of the crystals of pure materials, DIC-RAN, and the physical mixture. The samples were mounted on a double-sided carbon adhesive, coated with gold and processed in a standard sputter before observation in an LEO1450VP instrument (Carl Zeiss Microscopy AG, Oberköchen, Germany).

Nuclear Magnetic Resonance

NMR spectroscopy was used for the investigation of the interaction between DIC and RAN and the molar relationship of DIC-RAN. The ^1H and ^{13}C NMR spectra were acquired in MeOH-d_4 in a Bruker Avance spectrometer (Bruker BioSpin GmbH, Karlsruhe, Germany) with a magnetic field of 7.05 T, operating at 300.13 and 75.48 MHz for ^1H and ^{13}C, respectively. The NMR signals are abbreviated as follows: s = singlet; d = doublet; t = triplet; dd = doublet of doublets, dt = doublet of triplets, and b = broad signal. The chemical shifts (δ) are reported in parts per million downfield from tetramethylsilane, used as internal standard, and the coupling constants (*J*) are expressed in Hertz. The corresponding pulse programs were taken from the Bruker software library.

Sample Preparation for UV and Multivariate Curve Resolution-Alternating Least Squares Dissolution

Stock standard solutions of DIC-Na (108 ppm) and RAN·HCl (119 ppm) were independently prepared in 100-mL volumetric flasks, by dissolving accurately weighed amounts of the drugs in methanol. Three sets of 10 calibration samples each (5 for each API) were prepared in volumetric flasks, by transferring appropriate volumes of the stock solutions of the drugs and diluting to the mark with 0.1 M HCl, 0.1 M phosphate buffer, pH 5.8, and 0.1 M phosphate buffer, pH 6.8. The concentration levels obtained for DIC were 21.60, 16.20, 10.80, 5.40, and 2.16 ppm and those for RAN were 23.80, 17.85, 11.90, 5.95, and 2.38 ppm.

Online System for Dissolution and UV Measurements

The dissolution tests were carried out with a Hanson SR8-Plus dissolution test station (Hanson Research, Chatsworth, CA), configured with paddles (USP apparatus II).[29] The dissolutions were performed in 900 mL of 0.1 M HCl, 0.1 M phosphate buffer, pH 5.8, and 0.1 M phosphate buffer, pH 6.8, as dissolution medium and thermostatized at 37°C, at a paddle rotation rate of 50 rpm. The dissolution medium was degassed before use by sonication in a Cole Parmer 8891 ultrasonic bath (Cole Parmer, Vernon Hills, IL).

The UV spectroscopic determinations for monitoring drug dissolution were carried out with a Shimadzu UV-1601PC double-beam spectrophotometer (Shimadzu Corp., Kyoto, Japan) controlled by Shimadzu's UV-Probe (version 2.00) software and fitted with an 80-μL flow cell of 10-mm optical path length (Hellma, Müllheim, Germany). The determinations were performed against a blank of dissolution medium contained in a 10-mm optical path length quartz cuvette placed in the reference cell holder.

The dissolution medium was continuously withdrawn from the dissolution vessel through the sampling probe at a 1.5 mL min^{-1} flow rate, by means of a Gilson Minipuls 3 peristaltic pump and returned to the dissolution vessel after passing through the spectrophotometer flow cell. Degassing of the dissolution media and online sample filtration avoided potential interferences on account of bubbles or undissolved particles.

The UV spectra of the dissolution samples were collected after a standard pre-established delay time of 1.0 min, corresponding to the tubing dead volume. The dissolution experiments were monitored every 1.0 min during 2 h, and spectra were acquired at 1-nm intervals in the 245-400 nm range (156 data points per spectrum). The acquired data were saved as a matrix in comma-separated value (CSV) format.

For quantitative purposes, the calibration solutions of DIC-Na and RAN·HCl were sequentially pumped through the flow cell for periods of 5 min each, and 5 spectra per concentration level were collected. The full calibration data of each analyte were saved in CSV format, read into MATLAB, and stored as matrices ($D_{cDIC(25\times156)}$ and $D_{cRAN(25\times156)}$). The dissolution of the samples of DIC-RAN was monitored analogously.

Computational Methods

Chemometrics computations were carried out in MATLAB R2010a (Mathworks, Natick, MA), using MCR-ALS routines.[30] The full calibration data of each analyte were saved in CSV format, read into MATLAB, and stored as matrices ($D_{cDIC(25\times156)}$ and $D_{cRAN(25\times156)}$). The dissolution data of the samples of DIC-RAN were also stored in CSV format and read into MATLAB as a single matrix ($D_{t(120\times156)}$) for each dissolution experiment. The calculations were performed without special data preprocessing, using non-negativity of absorbances and concentrations as MCR-ALS constraints. Origin 8.5 (Origin Lab, Northampton, MA) was used for graphics and statistical data analyses.

Spectroscopic Data

Powder X-Ray Diagrams

For DIC: 2θ 10.9, 15.4, 17.9, 20.7, 21.7, 23.7, 24.6, 25.6, 26.1, 28.3, and 28.7.

For DIC-Na: 2θ 6.6, 8.5, 11.1, 15.1, 17.1, 19.8, 23.1, 23.5, 23.8, 24.1, 24.9, 25.8, 26.9, and 27.8.

For RAN·HCl: 2θ 8.4, 14.6, 15.3, 16.5, 18.1, 19.3, 20.3, 20.9, 23.5, 24.1, 25.9, 26.7, 27.5, 28.7, 31.9, and 33.0.

For DIC-RAN: 2θ 7.6, 11.4, 15.3, 19.2, 20.2, 20.6, 21.4, 25.6, 30.9, and 37.7.

Infrared Absorption

For DIC: 3323, 3080-2840, 2725-2563, 1694, 1587, 1577, 1568, 1508, 1480, 1454, 1422, 1413, 1322, 1305, 1282, 1273, 1251, 1200, 1160, 1093, 938, 890, 862, 837, 766, 752, 741, 710, 663, 630, and 610 cm^{-1}.

For DIC-Na: 3387, 3257, 3079, 3065, 3036, 2971, 1604, 1587, 1575, 1557, 1508, 1499, 1469, 1453, 1400, 1305, 1283, 1250, 1234, 1193, 1167, 1090, 1045, 952, 869, 845, 766, 747, 715, 670, and 636 cm^{-1}.

For RAN·HCl: 3257, 3189, 3097, 3013, 2995, 2975, 2948, 2910,2660, 2558, 2466, 1620, 1590, 1569, 1419, 1380, 1264, 1221, 1164, 1075, 1046, 1022, 1006, 992, 880, 761, and 700 cm^{-1}.

For DIC-RAN: 3285, 3197, 3155, 3135, 3067,1707, 1620, 1580, 1509, 1453,1380, 1304, 1250, 1202, 1154, 1036, 1010, 946, 871, 836, 793, 771, 757, 744, 715, 667, and 615 cm^{-1}.

Nuclear Magnetic Resonance

For DIC: (300 MHz, MeOH-d_4) δ 3.71 (s, 2H, $ArCH_2$), 4.85 (s, 2H, NH, and CO_2H), 6.40 (d, 1H, $J = 7.5$, H-3), 6.87 (dt, 1H, $J = 7.5$, H-5), 7.03 (dt, 1H, $J = 2.5$ and 7.5, H-4), 7.04 (t, 1H, $J = 8.0$, H-4′), 7.20 (dd, 1H, $J = 2.5$ and 7.5, H-6), and 7.39 (d, 2H, $J = 8.0$, H-3′, and H-5′).

For RAN·HCl: (300 MHz, MeOH-d_4) δ 2.81 (t, 1H, $J = 6.3$, H-12), 2.86 (s, 6H, H-8, and H-9), 2.90 (bs, 3H, H-17), 3.44 (t, 2H, $J = 6.3$, H-13), 3.84 (s, 2H, H-10), 4.36 (s, 2H, H-6), 4.87 (s, 3H, 3 × NH), 6.38 (d, 1H, $J = 3.2$, H-3), and 6.64 (d, 1H, $J = 3.2$, H-4). H-18 is missing due to H-D exchange with MeOH-d_4 during *E/Z* isomerization.[31]

For RAN: (300 MHz, MeOH-d_4) δ 2.25 (s, 6H, H-8, and H-9), 2.76 (t, 1H, $J = 6.3$, C-12), 2.89 (bs, 3H, H-17), 3.39 (t, 2H, $J = 6.3$, C-13), 3.51 (s, 2H, H-10), 3.79 (s, 2H, H-6), 4.86 (s, 3H, 3 × NH), and 6.24 (s, 2H, H-3, and H-4). H-18 is missing due to H-D exchange with MeOH-d_4 during *E/Z* isomerization.

For DIC-RAN: (300 MHz, MeOH-d_4) δ 2.72 (s, 6H, H-8, and H-9, RAN), 2.78 (t, 1H, $J = 6.3$, H-12, RAN), 2.88 (bs, 3H, H-17, RAN), 3.40 (t, 2H, $J = 6.3$, H-13, RAN), 3.71 (s, 4H, $ArCH_2$, DIC), 3.80 (s, 2H, H-10, RAN), 4.16 (s, 2H, H-6, RAN), 4.85 (s, 6H, NH, and OH), 6.33 (d, 1H, $J = 3.2$, H-3, RAN), 6.39 (d, 2H, $J = 7.5$, H-3, DIC), 6.52 (d, 1H, $J = 3.2$, H-4, RAN), 6.88 (dt, 2H, $J = 1.3$ and 7.6, H-5, DIC), 7.03 (dt, 2H, $J = 1.3$ and 7.6, H-4, DIC), 7.04 (t, 2H, $J = 7.8$, H-4′, DIC), 7.21 (dd, 2H, $J = 1.3$ and 7.6, H-6, DIC), and 7.38 (d, 4H, $J = 7.8$, H-3′ and H-5′, DIC). H-18 of RAN is missing due to H-D exchange with MeOH-d_4 during *E/Z* isomerization.

Results and Discussion

Preparation of DIC-RAN

Despite the literature precedent indicating the lack of interaction between DIC and RAN,[28] in our hands, the mixture of aqueous solutions of DIC-Na and RAN·HCl resulted in the precipitation of an off-white microcrystalline substance. The relative low yield of DIC-RAN obtained by the simple mixture of its precursors in water may be the result of the high aqueous solubility of the product, compared with the low solubility of DIC-Na, used for its generation. Although no efforts were performed to increase product yields, it is worthwhile noting that previous reports stated that no interaction took place when solutions of DIC-Na and RAN·HCl were mixed,[28] as it was aforementioned. On the other hand, careful manipulation of volumes and concentrations of the starting solutions, using the precursors in powder form and using antisolvents or co-solvents that favor the solubility of DIC-Na, relative to DIC-RAN, may result in increased yields.[32] However, these approaches should also bear in mind that NaCl is concomitantly produced, and operatively, it would be desirable to keep it in solution.

Thermal Characterization of DIC-RAN

The association of different thermal methods, including DSC, TGA, and HSM, made it possible to unveil details of the thermal behavior of DIC-RAN (Fig. 2). From the literature, it is known that the melting point of RAN is 69°C-70°C, whereas RAN·HCl melts at 134°C-140°C (form 1) or about 140°C-144°C (form 2), with decomposition.[5] On the other side, DIC melts at 156°C-158°C,[33] whereas DIC-Na has a melting point of 283°C-285°C.[2]

It was observed (Fig. 2a) that the melting point of DIC-RAN is associated with an endothermic DSC signal centered at 105.36°C (ΔH_m = 67.76 J g^{-1}). The event was also studied under an HSM, confirming its agreement with the melting of the sample and suggesting that a different phase was formed. The melt returned slowly to the solid state once cooled to room temperature, and no recrystallization peak was observed in the corresponding cooling curve (Fig. 2b).

In an extended temperature scale (Fig. 2d), the DSC thermogram revealed a complex pattern between 150°C and 375°C. In addition,

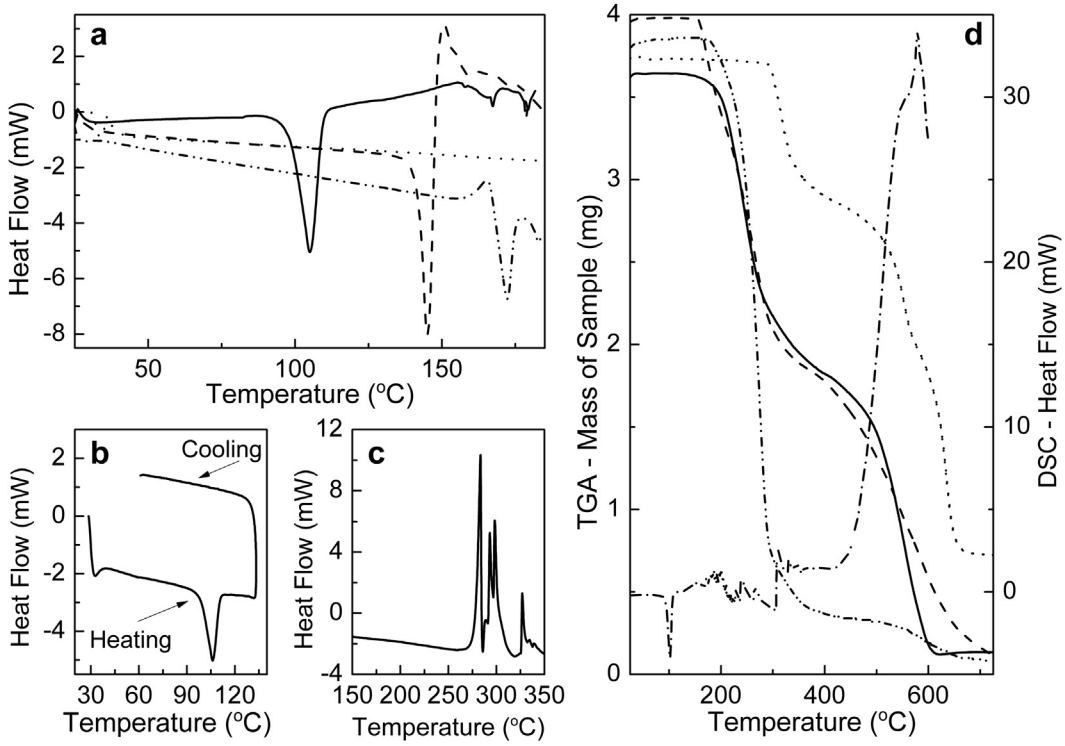

Figure 2. (a) DSC curves of RAN·HCl (—), DIC (-••-), DIC-Na (•••), and DIC-RAN (—) in the range 25°C-185°C; (b) DSC trace of DIC-RAN in the range 25°C-130°C; (c) DSC curve of DIC-Na in the range 150°C-350°C; and (d) TGA curves of RAN·HCl (—), DIC (-••-), DIC-Na (•••), and DIC-RAN (—) in the range 25°C-725°C and DSC trace of DIC-RAN (-•-).

an important exothermic process started >450°C, accounting for the final decomposition of DIC-RAN.

The TGA curve of DIC-RAN (Fig. 2d) confirmed the melting process because the initial mass remains stable up to 143°C, where decomposition begins to take place. Mass loss occurred in 2 decays without a stability plateau between them; at 660°C, DIC-RAN was completely degraded without leaving any solid residue.

DIC and DIC-Na melted as expected (Figs. 2a and 2d); both started to experience loss of mass between 170°C and 260°C, respectively; however, the mass loss of DIC-Na reached 82% at 680°C, the residue being NaCl, whereas the mass loss of DIC was complete at 650°C. Interestingly, it was observed that DIC undergoes dehydration when submitted to high temperatures, such as the conditions found in gas chromatography/mass spectrometry,[34] to afford a lactam, known as the related compound A of DIC (see Fig. 1).[35] Furthermore, this lactam has been shown to be formed during the thermal analysis of DIC-Na, in samples heated at 270°C.[36]

For the sake of comparison, it has been shown that RAN is stable up to 230°C; its thermogram evidences that it loses >20% of its weight when the temperature reaches 250°C.[37] On the other hand, RAN·HCl begins its decomposition at 158°C, and at 785°C, mass loss was complete (Fig. 2d).

Powder X-Ray Diffraction

The powder X-ray diffraction (PXRD) patterns of the pure DIC, DIC-Na, RAN·HCl, and DIC-RAN are shown in Figure 3; the diffractograms of the starting APIs are consistent with the literature.[38,39] The presence of characteristic reflections revealed that a new crystalline phase, different from those of the precursors, was obtained.

FTIR Characterization of DIC-RAN

To gain insight into interactions at the molecular level and detect the participating functional groups in both drugs, the spectra of DIC, DIC-Na, RAN·HCl, and DIC-RAN were comparatively examined (Fig. 4). Table 1 details the corresponding signals assignment for the spectra of DIC and RAN·HCl, which is consistent with the literature.

It has been observed that when DIC is involved in salt formation with an amine, the carbonyl peak appears <1675 cm^{-1}, whereas when the 2 components do not react, a composite of their individual IR spectra is produced and co-crystallization with hydrogen bond formation between the 2 components [O···H—N(heterocycle) or O—H···N(heterocycle)] generates a small shift of the carbonyl peak in the IR spectrum.[23]

The vibrational behavior of DIC-RAN (Fig. 4a) is clearly different from that of both APIs and of their physical mixture that merely consists of the superimposition of the isolated spectra of its precursors, thus evidencing the formation of a new entity. Furthermore, comparison between the DIC-RAN spectra obtained by the

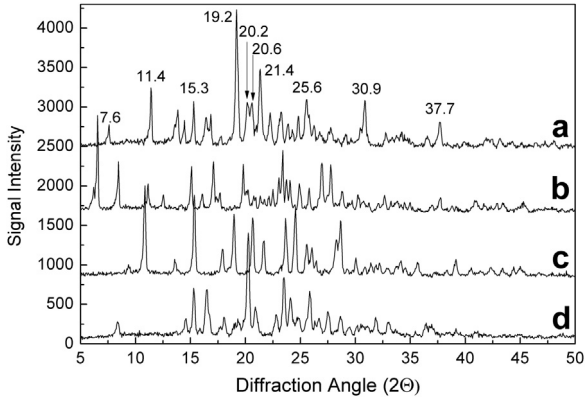

Figure 3. Stacked XRD patterns of (a) DIC-RAN, (b) DIC-Na, (c) DIC, and (d) form 2 of RAN·HCl.

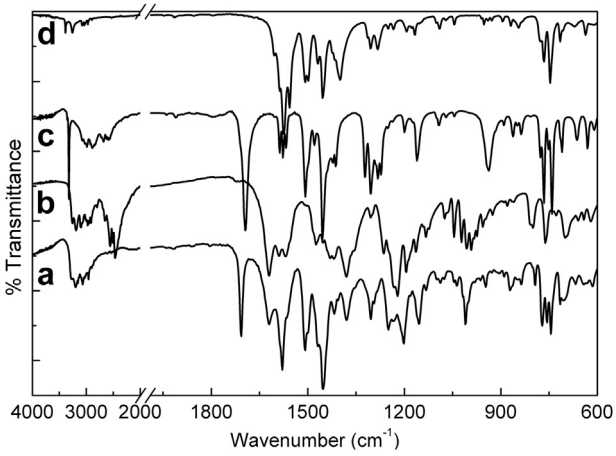

Figure 4. Stacked FTIR spectra of (a) DIC-RAN, (b) RAN·HCl, (c) DIC, and (d) DIC-Na.

DRIFTS and KBr pellet techniques ensured the absence of changes arising from compression during pellet preparation (see Supplementary Material).

The most striking changes in the FTIR spectrum of DIC-RAN were the modifications in the ν(N-H) modes. DIC-Na exhibits ν_{as}(N–H) and ν_s(N–H) signals at 3387 and 3257 cm^{-1},[36] respectively (Fig. 4d), whereas RAN·HCl (Fig. 4b) displays these modes as bands at 3257 and 3189 cm^{-1}.

However, DIC-RAN exhibits lower intensity bands shifted to 3155 and 3135 cm^{-1} and a 3285 signal (O-H stretch). In addition, the absence of the bands associated to the dimethylammonium group of RAN·HCl in the 2700-2250 cm^{-1} region was observed. Furthermore, the occurrence of a strong band at 1707 cm^{-1} [ν(C=O)], shifted 13 cm^{-1} to higher wave numbers with regard to DIC (1694 cm^{-1}), was also detected (Fig. 4c). In the solid state, DIC is strongly associated forming centrosymmetric dimers. The frequency of the carbonyl band of DIC-RAN [ν(C=O): 1707 cm^{-1}] is also typical to that of a dimerized carboxylic acid. However, compared with that found in the spectrum of DIC [ν(C=O): 1694 cm^{-1}], it is narrower in shape, of a lower intensity, and slightly shifted to higher wavenumbers, probably reflecting the different ability of DIC to become involved in inter- and intramolecular hydrogen bonding, due to its interaction with RAN, which lowers the stiffness of the C=O bond.

Analogous hypsochromic effects have been observed in other cases of co-crystal formation.[43] Moreover, it can be inferred that the lack of a strong N-H stretching signal, such as that found in DIC at 3325 cm^{-1}, may be indicative that the secondary amine group interacts more actively in DIC-RAN.

Taken together, all these findings suggested the presence of the carboxylic acid motif (-COOH; $\nu(C{=}O)_{DIC}$: 1694 cm^{-1}), instead of a carboxylate (-COO^-; $\nu(C{=}O)_{DIC\text{-}Na}$: 1575 cm^{-1}), most probably as a result of proton transfer from the protonated dimethylamino group of RAN, with the consequent formation of an associated species.

In the 1650-1300 cm^{-1} region, the main signals of DIC-RAN were different from those of the starting ingredients. The bands at 1620 cm^{-1} [ν(C=N), *aci*-nitro][40] and 1380 cm^{-1} [$\nu_s(NO_2)$] found in the spectra of both RAN·HCl and DIC-RAN revealed the presence of the nitronic acid tautomer, thus excluding the participation of this moiety in the interactions between DIC and RAN. Interestingly, however, the nitro moiety of RAN has been proposed to participate in interactions with the carboxylic acid motif of indomethacin.[44]

Furthermore, the spectrum of RAN·HCl form 2 displays 2 bands at 1590 and 1569 cm^{-1}, which can be attributed to the amidino moiety (N–C=N) of the nitroamidine.[44] However, in the DIC-RAN spectrum, these are replaced by a more intense, broad, and asymmetric band centered at 1580 cm^{-1}. Although it may be speculated that this peak is the result of an interaction at the amidine moiety, the complexity of the spectrum due to overlapping peaks in the 1570-1590 cm^{-1} region turn this into an inconclusive observation.

On the other hand, the peak at 1046 cm^{-1}, which has been specifically attributed to RAN·HCl form 2,[5] is shifted by 10 cm^{-1} to lower frequency in the DIC-RAN spectrum, confirming the presence of a different structure. Finally, DIC-RAN also exhibited bands at 871, 836, 771, 757, 744, and 715 cm^{-1} reminiscent of those found in DIC at analogous wavenumbers. These are characteristic of their 1,2-disusbtituted and 1,2,3-trisubstituted aromatic rings.

Nuclear Magnetic Resonance Analysis of DIC-RAN

The ^{1}H NMR spectrum of a molecule or a mixture of molecules provides valuable information about their structure and interactions with their environment. The chemical shifts provide clues on the sort of different chemical environments affecting the hydrogen atoms, whereas peak multiplicity reveals the number of coupled neighbor protons. On the other hand, the areas under the peaks of each group of equivalent protons are proportional to their relative molar abundances. Therefore, they yield the ratio of the numbers of hydrogen atoms in each of these environments.

Figure 5 exhibits the ^{1}H NMR spectra of DIC, RAN·HCl, RAN, and DIC-RAN in MeOH-d_4. Both components of the DIC-RAN species have different NMR characteristics in terms of their chemical shifts.

Table 1
Assignment of signals in the FTIR spectra of DIC and RAN·HCl

Diclofenac		Ranitidine·HCl	
Signal (ν, cm^{-1})	Attribution	Signal (ν, cm^{-1})	Attribution
3360-2560	ν(O–H), carboxylic acid	3257	ν_{as}(N–H)
3323	ν(>N–H)	3189	ν_s(N–H)
3080-2800	ν(C–H)	3097	ν(C–H), furan
1694	ν(C=O)	3013, 2995, 2975, 2948 and 2910	ν(C–H), aliphatic, ArH
1587	ν(C=C), aromatic rings	2660	ν(-N^+–HMe_2)
1568	ν(C=C), aromatic rings	2558	ν(-N^+–HMe_2)
1454	δ(CH_2)	1620	ν(C=N), nitronic acid[40]
1305	ν(C–N), Ar_2N	1590, 1569	ν(C=N), amidine (N–C=N)[a]
1282	ν(C–N), Ar_2N	1419	ν(N–Me)[41]
1200	δ(C–H), aromatic	1380	$\nu_{as}(NO_2)$[41]
1160	δ(C–H), aromatic	1221	$\nu_s(NO_2)$[41]
1093	ν(C–Cl)	1006	ν(N–C–C)[41]
862, 837, 766, 741 and 710	Substitution pattern of both aromatic rings		

[a] It has been suggested that this vibration, which usually takes place in the 1685–1580 cm^{-1} region, is displaced to lower wavenumbers in RAN because of the resonance and electron-withdrawing effect of the nearby nitro group.[42]

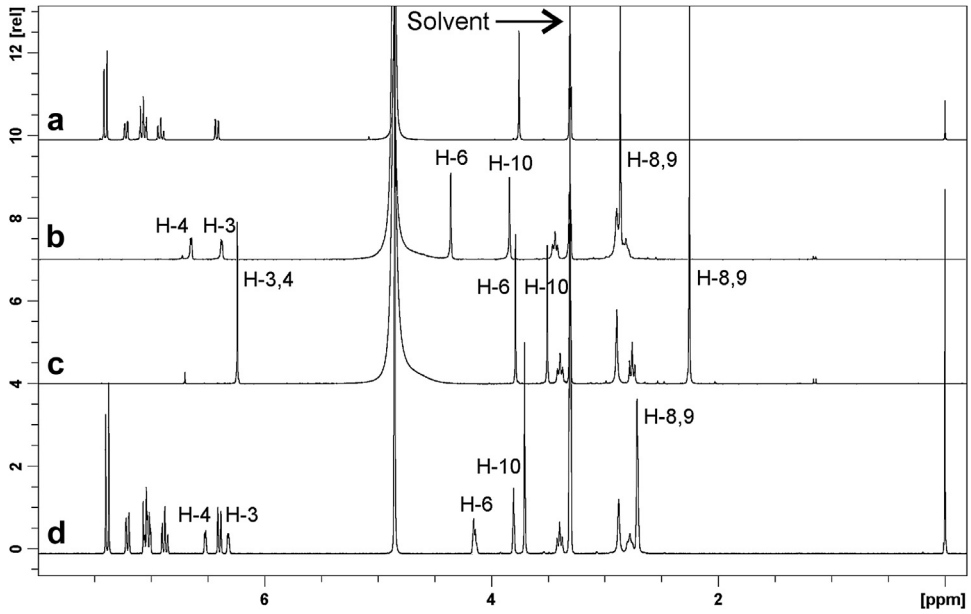

Figure 5. ^{1}H NMR spectra. (a) DIC, (b) RAN·HCl, (c) RAN, and (d) DIC-RAN, in MeOH-d_4.

Accordingly, the stoichiometry of the DIC-RAN co-crystal (ratio of DIC/RAN) can be easily determined by relating the areas of any 2 NMR signals as shown in Equation 1, one belonging to DIC (A_{DIC}) and the other to RAN (A_{RAN}), both of them normalized with regard to the number of protons responsible for giving rise to each one (N_{DIC} and N_{RAN}, respectively).

$$DIC/RAN = (A_{DIC} \times N_{RAN})/(A_{RAN} \times N_{DIC}) \quad (1)$$

Therefore, to establish the DIC/RAN stoichiometry in the DIC-RAN co-crystal, based on the assigned ^{1}H NMR spectra of the latter and its precursors, the downfield region of the spectrum was examined and the areas of the signals of H-3 of DIC ($\delta = 6.39$ ppm) and H-4 of RAN ($\delta = 6.52$ ppm) were compared. Because both were originated by single protons, their ratio (2:1) equaled the DIC/RAN stoichiometric ratio.

The same result was obtained when the upfield region was analyzed. In this case, the areas of the signals corresponding to the methylene protons of DIC ($\delta = 3.71$ ppm) and H-10 of RAN ($\delta = 3.80$ ppm) were related. Both signals are originated by pairs of equivalent protons; as a result, the DIC/RAN stoichiometry was derived directly from their ratio (2:1). Therefore, it can be unequivocally concluded that the DIC/RAN molar relationship in DIC-RAN is 2:1.

Interestingly, the signal of H-18 is missing from the spectra of RAN and DIC-RAN, probably due to tautomerization or *E/Z* isomerization of the double bond of the enamino tautomer of RAN, which takes place with concomitant H–D exchange with the deuterated NMR solvent. The formation of a 2:1 DIC-RAN heterotrimer, confirmed by NMR spectroscopy, is quite unexpected especially in view that the interaction between DIC and cetirizine, which has 2 protonable tertiary amino groups, was reported to afford the 1:1 heterodimeric compound.[28]

Comparing the signals of DIC-RAN with those of the pure compounds, it can be observed that the signals of DIC appeared, in general, 0.02-0.06 ppm downfield in the new substance with regard to the pure compound. However, the methylene protons next to the carboxylic acid moiety were the most affected ones.

Furthermore, the spectra of RAN and RAN·HCl are different as a consequence of the protonation of the *N,N′*-dimethylamino moiety of the drug. This is more evident in the signals of both methyls (H-8 and H-9) and the methylene group (H-6) bond to the nitrogen atom and in the protons attached to the furan ring (H-3 and H-4). For the singlets corresponding to the methyl groups in DIC-RAN, the signals ($\delta = 2.72$ ppm) look nearer to that of RAN·HCl ($\delta = 2.86$ ppm) than to that of RAN ($\delta = 2.25$ ppm). On the other hand, the resonances of H-6 were observed as singlets at $\delta = 4.36$ ppm in RAN·HCl and at $\delta = 4.16$ ppm in DIC-RAN, whereas in RAN they were found more shielded, at $\delta = 3.79$ ppm. Similarly, the resonances of H-3 and H-4 were observed as doublets in DIC-RAN ($\delta = 6.33$ and 6.52 ppm, respectively; $J = 7.5$ Hz) and in RAN·HCl ($\delta = 6.38$ and 6.64 ppm, respectively, $J = 3.2$), whereas in RAN they were detected as a more shielded singlet ($\delta = 6.24$ ppm). These findings further confirm that the *N,N′*-dimethylamino moiety is involved in an interaction with DIC. No other evidence of additional major perturbations could be gathered from these spectra.

The ^{13}C NMR analysis provided evidence pointing in the same direction. The spectra of RAN and RAN·HCl in MeOH-d_4 revealed subtle differences (see Supplementary Material), with the spectrum of DIC-RAN tending to agree more with that of RAN·HCl. On the other hand, the major differences between the spectra of DIC and DIC-RAN were found in the resonances of the CH_2CO_2H moiety.

Scanning Electron Microscopy

Representative SEM micrographs of DIC-Na, RAN·HCl, a physical mixture of these precursors, and DIC-RAN are shown in Figure 6. The morphology of the DIC-RAN crystals (Fig. 6d), observed as thin plates with a smooth surface, is clearly different from that of the product of a physical mixture (Fig. 6c) and differs from that of the APIs (Figs. 6a and 6b), confirming the formation of a new entity.

Physical and Chemical Stability

DIC-RAN proved to be thermally stable, not losing mass when heated up to 140°C; its chemical integrity was confirmed by FTIR because the spectra of the new compound, recorded before and after its melting, were coincident.

Furthermore, the ^{1}H NMR spectrum of an aged sample was demonstrated to contain only DIC and RAN, in the appropriate (2:1)

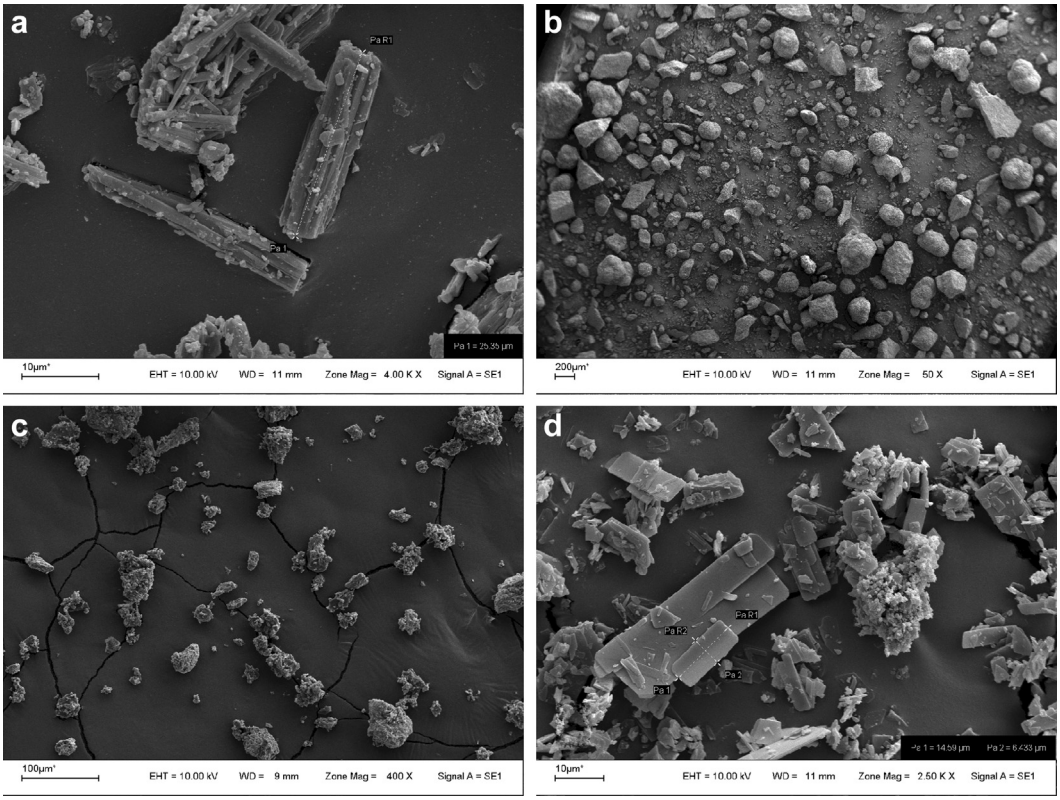

Figure 6. SEM micrographs of (a) DIC-Na, (b) RAN·HCl, (c) physical mixture of DIC-Na and RAN·HCl, and (d) DIC-RAN co-crystal.

proportions. No signs of thermally driven formation of impurities were observed. Furthermore, the thermal and vibrational behavior, and the structural features of the co-crystal remain unchanged at least 3 months at 20°C, as demonstrated by DSC, FTIR spectroscopy, and powder X-ray diffractometry.

Dissolution Testing

The dissolution performance of the analytes was evaluated at different pH values, analyzing their dissolutions from the pure drugs, their physical mixture, and from DIC-RAN.

The pharmaceutical dissolutions of the individual drugs (32.2 mg of DIC-Na and 17.7 mg of RAN·HCl), a physical mixture of DIC-Na and RAN·HCl (33.2 and 18.3 mg, respectively), and DIC-RAN (34.4 mg) were evaluated at pH 1.0, 5.8, and 6.8, using our previously reported online UV/MCR-ALS[45,46] approach to continuous dissolution monitoring.

Initially, pH 1 was chosen for its similarity to gastric pH. However, as expected, no relevant dissolution rates were found for DIC in both the physical mixture and DIC-RAN.

On the other hand, when pH 5.8 was used as dissolution medium, the dissolution of DIC reached levels of about 75% and 85% after 120 min, for the physical mixture and DIC-RAN, respectively, whereas the dissolution of RAN·HCl was near quantitative within 20 min.

Interestingly, it was observed that RAN·HCl dissolved faster than DIC-RAN. Conversely, the dissolution of DIC was faster when released from DIC-RAN. In addition, the shapes of the dissolution curves of DIC and RAN were similar when released from DIC-RAN, being in agreement with an intimal interaction among its components.

At pH 6.8, when the spectra and the dissolution curves were accessed through our MCR-ALS procedure, it was observed that the normalized spectra obtained from the ingredients of the physical mixture were highly correlated ($r^2 = 0.9998$ and 0.9999, $n = 156$), with those of the corresponding standards of DIC and RAN, measured under the same conditions (Fig. 7a).

Furthermore, examination of the dissolution curves of the pure drugs and those of their physical mixture (Fig. 7b) revealed that the API in the physical mixture dissolved independently from each other, their dissolution behavior being quite similar to that of the corresponding pure drugs. RAN·HCl dissolved almost quantitatively during the first 5 min, whereas it took >90 min for DIC to arrive to a complete dissolution. This information is indicative that the observed dissolution enhancement is a result of a solid-state interaction and not a co-operative phenomenon between both drugs in solution, under the experimental conditions.

The dissolution curves obtained after the MCR-ALS deconvolution exhibited a synchronized release for both drugs, which was significantly faster than the DIC as an individual component.

Next, the dissolution of DIC-RAN was examined under similar conditions. The MCR-ALS algorithm, run with 120 spectra per dissolution of each analyte and under restrictions of non-negativity in the absorbances and concentrations, provided the normalized spectra of DIC and RAN, and the dissolution curves of both APIs alone and from the DIC-RAN sample (Figs. 7c and 7d). Comparison of the additive UV spectrum (DIC + RAN, 2+1) with the spectrum of a dissolution sample (Fig. 7c) demonstrated that both were highly correlated ($r^2 = 0.9997$, $n = 156$).

On the other hand, as shown in Figure 7d, the dissolution of DIC-RAN was complete within 5 min for both DIC and RAN. Both curves exhibited synchronized dissolution behavior, being simultaneously delivered from the solid in a given molar relationship, which was determined from UV measurements as 1.9:1. Even though this value falls slightly apart from the ratio obtained by ^{1}H NMR signal integration (2:1), it is satisfactory as an alternative and

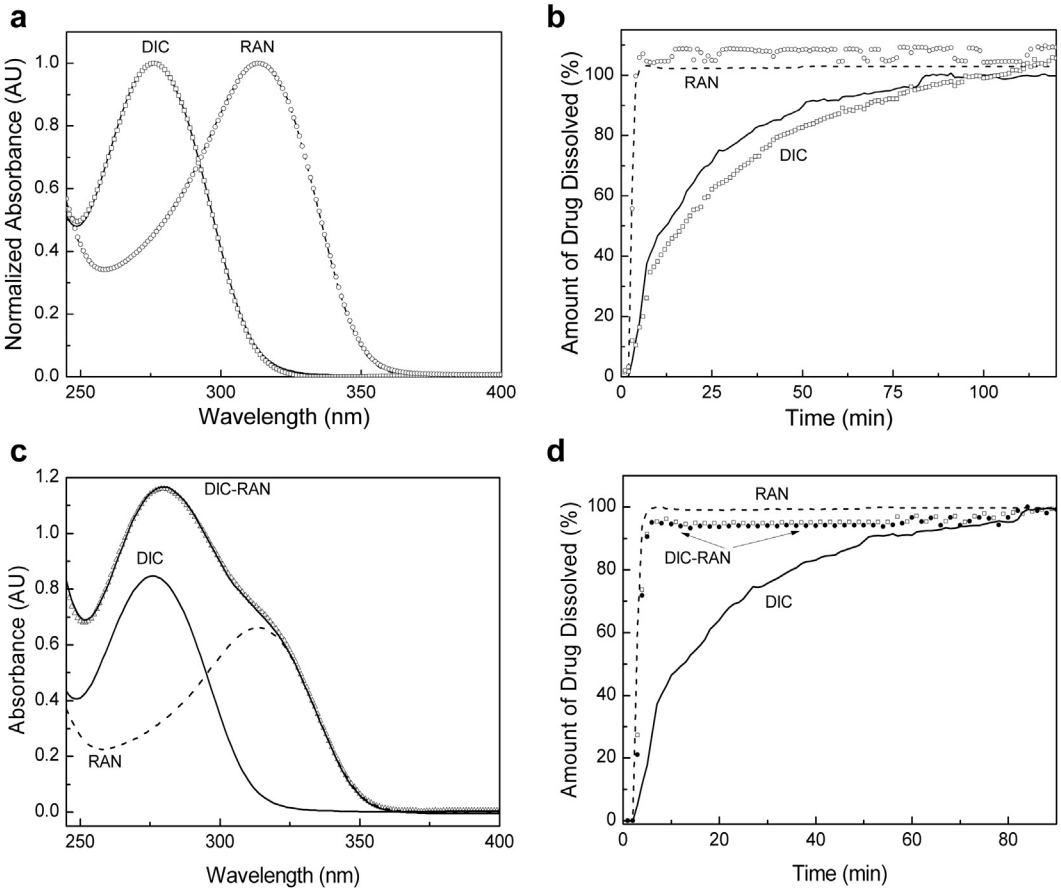

Figure 7. (a) Normalized spectra of DIC (——) and RAN (——) and MCR-ALS output spectra of DIC (□) and RAN (○); (b) dissolution curves of pure DIC (——) and RAN (——) and dissolution of a physical mixture of DIC (□) and RAN (○); (c) normalized spectra of DIC and RAN obtained as the MCR-ALS output from the dissolution of DIC-RAN. Comparison of the additive (2 + 1) spectra of the drugs with that of DIC-RAN (Δ); and (d) dissolution curves of pure DIC (——) and RAN (——) and of the same drugs [DIC (□) and RAN (●)] from DIC-RAN.

independent determination of the molar relationship of the components of DIC-RAN.

This result indicated that, opposite to the physical mixture, a strong relationship between DIC and RAN, of chemical origin, is present in DIC-RAN. This kind of phenomena has been linked to drug-drug interactions resulting from the formation of hetero-oligomers.[47,48]

Additionally, the dissolution curves of RAN and DIC in DIC-RAN are almost superimposable to that of RAN·HCl, suggesting that the dissolution rate of the new compound is governed by RAN. This outcome is advantageous from the pharmaceutical technology point of view because it affords a significant improvement in the dissolution rate of DIC.

Heterotrimer Formation

In view of these results, it can be assumed that the changes in the dissolution behavior of DIC are a consequence of the formation of a heterotrimeric product with RAN. Being highly soluble, through this interaction, RAN would impose an improved dissolution rate for DIC from DIC-RAN.

RAN has 2 basic groups with p*K*a values of 2.3 and 8.2,[49] which means that it can accept >1 proton; however, between pH 4 and 7, it should exist primarily as a monovalent cation. It has been shown that on addition of HCl to RAN, the first equivalent of the acid serves to protonate the nitrogen atom of the alkyldimethylamino group. As the pH decreases, the second equivalent of HCl reacts with the ethenediamine moiety, causing a *C*-protonation rather than an *N*-protonation.[50]

On the other hand, the p*K*a of the carboxylic acid moiety of DIC is 3.80, which means that it can protonate the alkyl-*N,N′*dimethylamino moiety of RAN to a certain extent; on the contrary, the p*K*b of the N-H in DIC is 10, meaning that it would not be readily deprotonated.

Unfortunately, suitable crystals of DIC-RAN could not be obtained to fully ascertain its structure by single crystal X-ray diffractometry. However, somehow reminiscing the indomethacin-saccharin co-crystal,[51] and despite RAN tautomerism may be the cause of a more complex picture, a working model-like structure shown in Figure 8 can be proposed for the heterotrimer.

In this model, the acid dimer of DIC in the asymmetric unit displays a weak N···H–O interaction with the alkyl-*N,N′*dimethylamino moiety of RAN (acid–dimethylamino heterosynthon). In addition, the DIC molecules are connected to each other through a hydrogen bond network that involves an O–H···O motif and as much as a couple of stabilizing weak intermolecular N–H···O interactions (alternatively, some of the latter may be intramolecular in nature).

This arrangement, where the carbonyls have less restricted vibrational motion, explains the presence of a single peak for this group in the infrared spectrum of DIC-RAN and accounts for its narrow shape and shift toward higher wavenumbers. Furthermore, as a result of partial opening of the acid synthon of DIC within the co-crystal, it can be foreseen that the solubility of the latter would be improved and, at the time of the dissolution, further dissociation

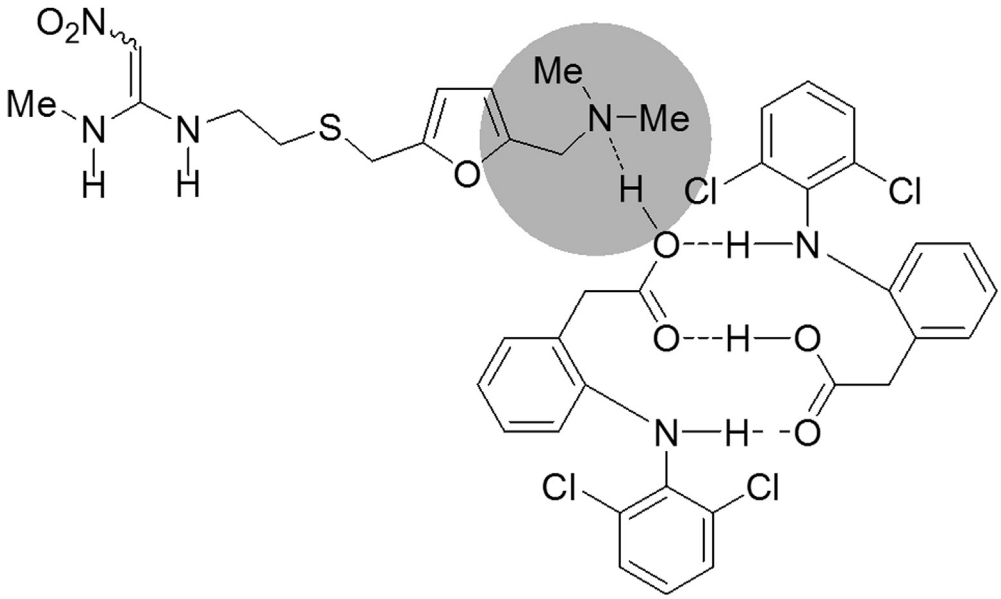

Figure 8. Proposed working model for the structure of the DIC-RAN unit, showing hydrogen bonds between 2 molecules of DIC and 1 molecule of RAN. The main interaction site is highlighted.

of the acid moiety could take place, favored by the high dielectric constant of the aqueous medium.

In this working picture, additional N—H···O contacts between the amidine moiety of RAN and the carbonyl motif of a neighboring DIC molecule cannot be fully excluded. The latter intermolecular interactions may play a considerable role in stabilization of the supramolecular unit to form crystals.

Pharmacologically relevant combinations of 2 drugs have been used for the preparation of co-amorphous systems as promising candidates for formulations intended for combination therapy.[52] Despite that the combination of DIC and RAN is a pharmaceutically relevant association and that RAN meets the conditions of a suitable salt formation agent,[53] the typical daily doses of DIC and RAN are in the ranges 50-150 and 150-300 mg, respectively.

The delivery of 150 mg of DIC through the intermediacy of DIC-RAN would supply approximately 75 mg of RAN. However, because the dose of the latter can be supplemented in a drug formulation, the feasibility of using DIC-RAN as part of a form of co-administration of DIC and RAN should not be ruled out.

Conclusions

The formation of DIC-RAN was observed on mixing aqueous solution of DIC-Na and RAN·HCl. The solid was characterized by microscopic, diffractometric, thermal, and spectroscopic methods, including SEM, PXRD, DSC, TGA, FTIR, and NMR. DIC-RAN was demonstrated to be a thermally stable binary drug system that melts around 105°C, in which the presence of DIC and RAN in a 2:1 molar ratio was unequivocally confirmed by NMR spectroscopy and UV-chemometrics studies. On the other hand, the spectral evidence allowed the identification of the main groups involved in interactions between the molecular species. It was suggested that DIC-RAN has a 3-component supramolecular unit, which consists of an intermolecular hydrogen-bonded centrosymmetric DIC dimer associated with a molecule of RAN. The ingredients of DIC-RAN dissolved synchronically, thus providing an improved dissolution behavior for DIC, and evidencing that an interaction takes place between them.

Acknowledgments

The authors thank Consejo Nacional de Investigaciones Científicas y Tecnológicas (CONICET, PIP 2012-0471), Agencia Nacional de Promoción Científica y Tecnológica (ANPCyT, PICT 2011-0399, PICT 2012-1994), Secretaría de Ciencia y Técnica de la UNSL (PROICO 2-1612), and Secretaría de Ciencia y Tecnología de la UNR (SECyT-UNR, BIO-300) for financial support. NLC and ROG are also thankful to CONICET and CIN, respectively, for their fellowships.

References

1. Chiarini A, Tartarini A, Fini A. pH-solubility relationship and partition coefficients for some anti-inflammatory arylaliphatic acids. *Arch Pharm (Weinheim)*. 1984;317:268-273.
2. Adeyeye CM, Li PK. Diclofenac sodium. In: Florey K, ed. *Analytical Profiles of Drug Substances*. Vol. 19. NJ: Academic Press; 1990:123-144.
3. Dhaked DK, Bharatam PV. Nitro ↔ aci-nitro tautomerism and *E/Z* isomeric preferences of nitroethenediamine derivatives: a quantum chemical study. *RSC Adv*. 2013;3:25268-25277.
4. Calvo NL, Simonetti SO, Maggio RM, Kaufman TS. Thermally induced solid-state transformation of cimetidine. A multi-spectroscopic/chemometrics determination of the kinetics of the process and structural elucidation of one of the products as a stable N3-enamino tautomer. *Anal Chim Acta*. 2015;875:22-32.
5. Mirmehrabi M, Rohani S, Murthy KSK, Radatus B. Characterization of tautomeric forms of ranitidine hydrochloride: thermal analysis, solid-state NMR, X-ray. *J Cryst Growth*. 2004;260:517-526.
6. Crisponi G, Cristiani F, Nurchi VM, et al. A potentiometric, spectrophotometric and ^{1}H NMR study on the interaction of cimetidine, famotidine and ranitidine with platinum(II) and palladium(II) metal ions. *Polyhedron*. 1995;14:1517-1530.
7. Aaltonen J, Rades T. Towards physico-relevant dissolution testing: the importance of solid-state analysis in dissolution. *Dissol Technol*. 2009;16:47-54.
8. Lobmann K, Laitinen R, Grohganz H, Strachan C, Rades T, Gordon KC. A theoretical and spectroscopic study of coamorphous naproxen and indomethacin. *Int J Pharm*. 2013;453:80-87.
9. Serajuddin ATM. Salt formation to improve drug solubility. *Adv Drug Deliv Rev*. 2007;59:603-616.
10. O'Connor KM, Corrigan OW. Preparation and characterization of a range of diclofenac salts. *Int J Pharm*. 2001;226:163-179.
11. Fini A, Cavallari C, Ospitali F. Diclofenac salts. V. Examples of polymorphism among diclofenac salts with alkyl-hydroxy amines studied by DSC and HSM. *Pharmaceutics*. 2010;2:136-158.
12. Báthori N, Lemmerer A, Venter G, Bourne S, Caira M. Pharmaceutical co-crystals with isonicotinamide—vitamin B3, clofibric acid, and diclofenac—and two isonicotinamide hydrates. *Cryst Growth Des*. 2011;11:75-87.
13. Fini A, Fazio G, González-Rodríguez M, Cavallari C, Passerini N, Rodríguez L. Formation of ion-pairs in aqueous solutions of diclofenac salts. *Int J Pharm*. 1999;187:163-173.

14. Dias MMR, Raghavan SL, Pellett MA, Hadgraft J. The effect of β-cyclodextrins on the permeation of diclofenac from supersaturated solutions. *Int J Pharm*. 2003;263:173-181.
15. Khan MA, Chourasia A. Mixed solvency approach- boon for solubilization of poorly water soluble drug diclofenac sodium. *Res J Pharm Biol Chem Sci*. 2012;3:865-868.
16. Khan MA. Enhancement of solubility of poorly water soluble drugs diclofenac sodium by mixed solvency approach. *Int J Res Dev Pharm Life Sci*. 2013;2:580-582.
17. Vajir S, Sahu V, Ghuge N, Bang P, Bakde BV. Enhancement of dissolution rate of poorly water soluble diclofenac sodium by liquisolid technique. *Int J Pharm Chem Sci*. 2012;1:1338-1349.
18. Pavan Kumar KH, Chandramouli Y, Prakash Reddy CS, Sreekanth K, Murali D, Chakravarthi RN. Enhancement of solubility and dissolution rate of diclofenac sodium by solid dispersion method. *Int J Adv Pharm*. 2012;2:110-118.
19. Lai F, Sinico C, Ennas G, Marongiu F, Marongiu G, Fadda AM. Diclofenac nanosuspensions: influence of preparation procedure and crystal form on drug dissolution behavior. *Int J Pharm*. 2009;373:124-132.
20. Fanun M. Conductivity, viscosity, NMR and diclofenac solubilization capacity studies of mixed nonionic surfactants microemulsions. *J Mol Liq*. 2007;135:5-13.
21. Gubbins RH, O'Driscoll CM, Corrigan OI. The effects of casein on diclofenac release from hydroxypropylmethylcellulose (HPMC) compacts. *Int J Pharm*. 2003;260:69-76.
22. O'Connor KM, Corrigan OI. Comparison of the physicochemical properties of the *N*-(2-hydroxyethyl)pyrrolidinediethylamine and sodium salt forms of diclofenac. *Int J Pharm*. 2001;222:281-293.
23. Aakeröy CB, Grommet AB, Desper J. Co-crystal screening of diclofenac. *Pharmaceutics*. 2011;3:601-614.
24. Alioth C, Blum RA, D'Andrea DT, et al. Application of dual radiotelemetric technique in studying drug-drug interaction between diclofenac sodium and ranitidine HCl in volunteers. *Pharm Res*. 1993;10:1688-1692.
25. Leucuta A, Vlase L, Farcau D, Nanulescu M. No effect of short term ranitidine intake on diclofenac pharmacokinetics. *Roman J Gastroenterol*. 2004;13:305-308.
26. Shirse P. Formulation and evaluation of bilayer tablets of diclofrenac sodium with ranitidine HCl for sustained and immediate release. *J Appl Pharm Sci*. 2012;2:136-141.
27. Carrasco-Portugal MC, Aguilar-Cota ME, Pérez-Urlzar J, Cabrera O, Herrera JE, Flores-Murrieta FJ. Bioavailability of a formulation containing a diclofenac-ranitidine combination. *Proc West Pharmacol Soc*. 2002;45:8-10.
28. Kenawi IM, Barsoum BN, Youssef MA. Drug–drug interaction between diclofenac, cetirizine and ranitidine. *J Pharm Biomed Anal*. 2005;37:655-661.
29. The United States Pharmacopeia, USP35–NF30. *Dissolution Procedure: Development and Validation, U. S*. Rockville, MD, USA: Pharmacopeial Convention Inc.; 2011 Chapter 1092.
30. Jaumot J, Gargallo R, de Juan A, Tauler RA. Graphical user-friendly interface for MCR-ALS: a new tool for multivariate curve resolution in MATLAB. *Chemom Intell Lab Syst*. 2005;76:101-110.
31. Gaggelli E, Marchettini N, Sega A, Valensin G. Conformation and dynamics of ranitidine in solution as detected by ^{1}H and ^{13}C NMR spectroscopy. *Magn Reson Chem*. 1988;26:1041-1046.
32. Lee M-J, Chun N-H, Wang I-C, Liu JJ, Jeong M-Y, Choi GJ. Understanding the formation of indomethacin–saccharin cocrystals by anti-solvent crystallization. *Cryst Growth Des*. 2013;13:2067-2074.
33. Goh CF, Lane ME. Formulation of diclofenac for dermal delivery. *Int J Pharm*. 2014;473:607-616.
34. El Haj BM, Al Ainri AM, Hassan MH, Bin Khadem RK, Marzouq MS. The GC/MS analysis of some commonly used non-steroidal anti-inflammatory drugs (NSAIDs) in pharmaceutical dosage forms and in urine. *Forens Sci Int*. 1999;105:141-153.
35. Vignaduzzo SE, Castellano PM, Kaufman TS. Experimentally designed, validated HPLC simultaneous determination of pridinol and diclofenac in their combined pharmaceutical formulations, which allows limiting diclofenac related compound A. *J Liq Chromatogr Relat Technol*. 2010;33:1720-1732.
36. Tudja P, Khan MZI, Mestrovic E, Horvat M, Golja P. Thermal behaviour of diclofenac sodium: decomposition and melting characteristics. *Chem Pharm Bull*. 2001;49:1245-1250.
37. Novoa De Armas H, Peeters OM, Blaton N, et al. Solid state characterization and crystal structure from X-ray powder diffraction of two polymorphic forms of ranitidine base. *J Pharm Sci*. 2009;98:146-158.
38. Palomo ME, Ballesteros MP, Frutos P. Analysis of diclofenac sodium derivatives. *J Pharm Biomed Anal*. 1999;21:83-94.
39. Madan T, Kakkar AP. Preparation and characterization of ranitidine-HCl crystals. *Drug Dev Ind Pharm*. 1994;20:1571-1588.
40. Hohnjec M, Kuftinec J, Malnar M, et al. Ranitidine. In: Florey K, ed. *Analytical Profiles of Drug Substances*. Vol. 15. New York, NY: Academic Press; 1986:533-562.
41. Sovilj SP, Dzambaski A, Jovanovic T. Novel Cu(II) complexes with ranitidine and nizatidine. *Asian J Chem*. 2003;15:19-24.
42. Colthup NB, Daly LH, Wiberley SE. *Introduction to Infrared and Raman Spectroscopy*. 3rd ed. San Diego, CA: Academic Press; 1990.
43. Basavoju S, Boström D, Velaga SP. Indomethacin–saccharin cocrystal: Design, synthesis and preliminary pharmaceutical characterization. *Pharm Res*. 2008;25:530-541.
44. Chieng N, Aaltonen J, Saville D, Rades T. Physical characterization and stability of amorphous indomethacin and ranitidine hydrochloride binary systems prepared by mechanical activation. *Eur J Pharm Biopharm*. 2009;71:47-54.
45. Calvo NL, Maggio RM, Kaufman TS. An eco-friendly strategy, using on-line monitoring and dilution coupled to a second-order chemometric method, for the construction of dissolution curves of combined pharmaceutical associations. *J Pharm Biomed Anal*. 2014;89:213-220.
46. Maggio RM, Rivero MA, Kaufman TS. Simultaneous acquisition of the dissolution curves of two active ingredients in a binary pharmaceutical association, employing an on-line circulation system and chemometrics-assistance. *J Pharm Biomed Anal*. 2013;72:51-58.
47. Alleso M, Chieng N, Rehder S, Rantanen J, Rades T, Aaltonen J. Enhanced dissolution rate and synchronized release of drugs in binary systems through formulation: amorphous naproxen–cimetidine mixtures prepared by mechanical activation. *J Control Rel*. 2009;136:45-53.
48. Löbmann K, Laitinen R, Grohganz H, Gordon KC, Strachan C, Rades T. Coamorphous drug systems: enhanced physical stability and dissolution rate of indomethacin and naproxen. *Mol Pharm*. 2011;8:1919-1928.
49. Dumanovic D, Juranic I, Dzeletovic D, Vasic VM, Jovanovic J. Protolytic constants of nizatidine, ranitidine and *N,N*-dimethyl-2-nitro-1,1-ethenediamine, spectrophotometric and theoretical investigation. *J Pharm Biomed Anal*. 1997;15:1667-1678.
50. Cholerton TJ, Hunt JH, Klinkert G, Smith MM. Spectroscopic studies on ranitidine: Its structure and the influence of temperature and pH. *J Chem Soc Perkin Trans*. 1984;2:1761-1766.
51. Qiao N, Li M, Schlindwein W, Malek N, Davies A, Trappitt G. Pharmaceutical cocrystals: an overview. *Int J Pharm*. 2011;419:1-11.
52. Löbmann K, Strachan C, Grohganz H, Rades T, Korhonen O, Laitinen R. Coamorphous simvastatin and glipizide combinations show improved physical stability without evidence of intermolecular interactions. *Eur J Pharm Biopharm*. 2012;81:159-169.
53. Saal C, Becker A. Pharmaceutical salts: a summary on doses of salt formers from the Orange Book. *Eur J Pharm Sci*. 2013;49:614-623.